Hindawi
Advances in Civil Engineering
Volume 2024, Article ID 2980358, 14 pages
https://doi.org/10.1155/2024/2980358

Research Article

A Numerical Study on the Influence of Bolt Corrosion on the Long-Term Behavior of Steel–Concrete Composite Beams

Yalei Niu, Chen Qu, and Qingxing Feng

School of Civil Engineering and Architecture, Zhejiang University of Science and Technology, Hangzhou, Zhejiang, China

Correspondence should be addressed to Chen Qu; 103003@zust.edu.cn

Received 10 November 2023; Revised 17 March 2024; Accepted 20 April 2024; Published 13 May 2024

Academic Editor: Edén Bojórquez

This study establishes a numerical model for beam-type steel–concrete composite specimens considering the corrosion of anchor bolts, with which studies the long-term deformation performance of the components under sustained load. The experimental results were compared with the calculated values obtained by combining the effective modulus method according to the CEB-FIP 1990 code and the ACI 209R code. Then a comparison with the calculation method of shrinkage and creep in standards (Standard Creep Method (SCM)) is made, and it shows that by supplementing the degradation of interface stiffness due to corrosion (using the defined modulus method (DMM)), the simulation results match better with the experimental results, confirming that this approach is suitable for analyzing the long-term load conditions of anchor bolt corrosion. Furthermore, based on the defined modulus method, the long-term behavior of composite beams under different loads and varying corrosion rates is studied.

1. Introduction

Steel–concrete composite bridges built in China during the early stages, which have been in service for nearly 30 years, have entered the first phase of their life cycle. They are starting to experience material degradation, corrosion, and structural damage due to accidents, all of which affect the durability of steel–concrete composite beam bridges. The issue of long-term load-carrying capacity degradation caused by bolt corrosion has gradually become apparent. Composite beams can be classified into external concrete composite beams and T-shaped composite beams according to their cross-sectional forms (Figure 1), with T-shaped composite beams being commonly used.

Wang et al. [1] conducted a long-term experiment on a steel–concrete composite beam and used finite element simulation analysis to simulate the long-term behavior of concrete using three methods: concrete material creep function, effective modulus method, and adjusted shear stiffness at steel–concrete interface. They proposed a calculation method for long-term deflection of composite beams. Ji et al. [2] derived a deflection calculation formula for steel–concrete composite beams under long-term loading by considering the interlayer slip effect between steel beams and concrete deck slabs, full-section shear deformation of steel–concrete composite beams, and shrinkage creep effect of concrete deck slabs. The derived formula was validated against experimental and finite element results, showing that the shrinkage creep effect of concrete has a significant influence on the deflection of steel–concrete composite beams. Han [3] analyzed the effects of concrete creep and shrinkage in composite beams on stress distribution and structural behavior. Through a combination of analytical calculation, numerical simulation, and experimental analysis, they derived analytical formulas for stress redistribution caused by internal constraints in statically determinate and hyperstatic composite beam sections, as well as direct calculation formulas for the time-varying stress of composite beams. They obtained a series of accurate and approximate solutions. Fan et al. [4, 5] studied the effects of concrete shrinkage creep and cracking on the long-term mechanical performance of composite beams. Their experiments showed that both long-term loading under negative bending moment and concrete shrinkage effect lead to concrete cracking and inhibit the creep deformation of concrete. Di [6] studied the influence of concrete shrinkage creep on the long-term performance of steel–concrete composite bridges by establishing a finite element analysis

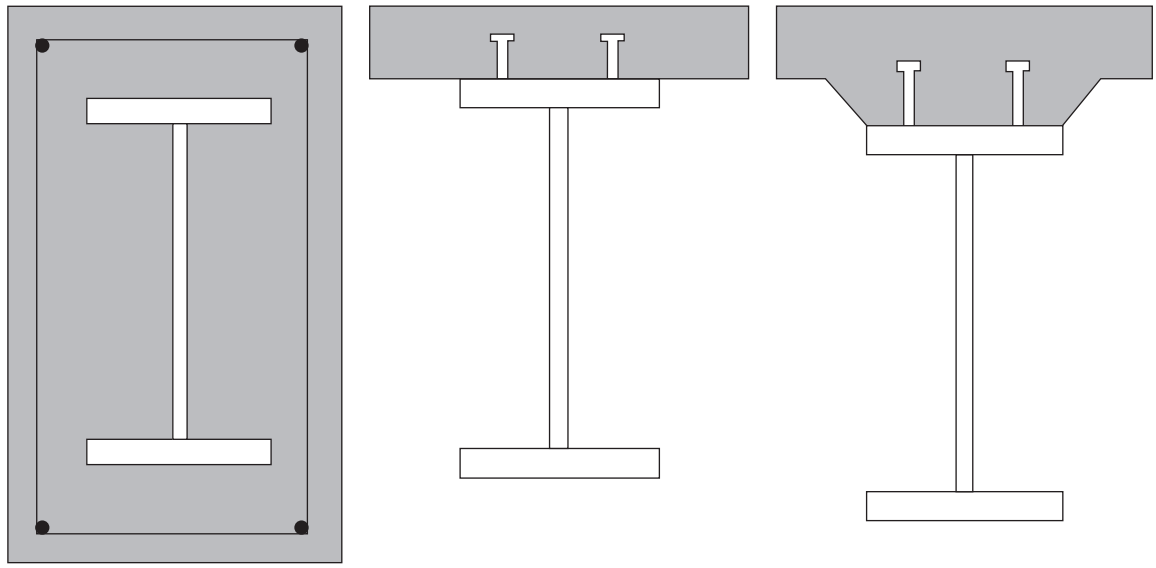

Figure 1: Different cross-sectional forms of composite beams. (a) Concrete encased steel composite beams. (b) T-shaped composite beam without flange plate. (c) T-shaped composite beam with flange plate.

model. They analyzed and researched three parameters that affect the concrete shrinkage creep effect, providing reference value for the design and construction of steel–concrete composite bridges regarding the impact of concrete shrinkage creep effect. Zhang [7] used the finite element method to study the models of steel–concrete composite beams with different bolt corrosion rates. They proposed calculation formulas for the flexural bearing capacity and stiffness of corroded bolt steel–concrete composite beams. Xiong et al. [8] conducted experimental tests on eight standard connection members to study the static properties of corroded bolt connections after long-term loading and unloading, as well as the effects of corrosion and loading. They established calculation formulas for the shear bearing capacity of corroded bolt connections and the load–slip curve. Peng [9] studied the long-term performance of composite beams under the combined effects of load and bolt corrosion through long-term experiments. They proposed a time-varying formula for the long-term deflection of steel–concrete composite beams. Here are the latest research findings from scholars in 2023. Xiao [10] and others conducted experiments on single-sided specimens to study the static performance of welded nail connections under different degrees of corrosion. The results indicate that the mechanical performance of welded nail connections decreases with corrosion, leading to degradation in composite structural performance and reduced durability. Based on the experimental results, they fitted coefficient curves and proposed a calculation formula for the shear bearing capacity of corroded welded nail connections. Wang et al. [11] conducted numerical simulations by establishing ABAQUS finite element models to study the degradation law of shear performance of bolted connections under different rust distribution patterns. The results indicate that under the same rust depth conditions, as the rust height increases, the shear carrying capacity of the bolt decreases; under the same rust height conditions, as the rust depth increases, the shear carrying capacity and stiffness exhibit a linear decreasing trend; and under the same rust height and depth conditions, the shear carrying capacity and stiffness decrease most significantly due to uniform circular rust. Wang [12] studied the effects of severe corrosion on the mechanical properties of steel–concrete composite girder bridges. Through experiments, numerical analysis, and theoretical analysis, he primarily investigated the degradation law of mechanical properties after corroding the steel bars with industrial hydrochloric acid and the failure modes and shear bearing capacity of PBL shear connectors, as well as the influence of various factors on the shear bearing capacity of shear connectors, and proposed corresponding formulas and models. Wang et al. [13] investigated the influencing factors of the bending capacity of steel–concrete composite beams after corrosion and fatigue and established a calculation method based on fracture mechanics and fatigue residual strength theory. The results indicate that the corrosion rate of bolts, concrete strength, fatigue loading limit, and number of bolts are the main factors affecting the bending capacity of composite beams. You et al. [14] studied the long-term performance of continuous steel–concrete composite beams considering the effects of concrete shrinkage and creep. Using ABAQUS software, he established a finite element model and verified the reliability of the simulation results. Additionally, he conducted a parameter analysis on the influence of recycled coarse aggregates on the long-term performance of these beams. The study found that using the age-adjusted effective modulus method and considering the temperature field to account for concrete shrinkage effects can accurately simulate the long-term performance of composite beams. The incorporation of recycled coarse aggregates increases deflection to a certain extent, and different floor types should adopt different shrinkage and creep models. Zhang et al. [15] conducted a 4-year field test to investigate

Table 1: Material parameters of reinforcement, steel sections, and bolt.

	Material	Dimension (mm)	Elastic modulus (Mpa)	Yield strength (Mpa)	Ultimate strength (Mpa)
Test	H-shaped steel	$125 \times 125 \times 6.5 \times 9$	2.01×10^5	317.4	434.1
	Bolt	13×16	2.11×10^5	325.7	414.6
	Reinforcement	$\Phi 6$	1.96×10^5	306.4	437.8
Standard	H-shaped steel	$125 \times 125 \times 6.5 \times 9$	2.1×10^5	235	370
	Bolt	13×16	—	320	400
	Reinforcement	$\Phi 6$	2.1×10^5	235	370

Note: The specific values for each parameter will be provided in the research report or can be obtained from relevant sources.

the temperature, shrinkage, and creep effects on steel–concrete composite girder bridges. Temperature field models (TFM) and mechanical behavior models (MBM) were verified and showed minor differences throughout the service stage. The study highlights the influence of meteorological factors on long-term behaviors of such bridges. Nan et al. [16] investigated the widespread application and economic benefits of steel–concrete continuous composite beams in buildings and bridges. Through a combination of elastic theory and numerical simulations, the study delved into the influence of slip and creep effects under long-term loads on structural performance, emphasizing the importance of considering the interaction between slip and creep. Zhao et al. [17] proposed a beam finite element model considering slip, shear lag, and time-dependent effects in steel–concrete composite box beams. The model employs a step-by-step method for time variable solutions, more accurate than the single-step algebraic method. Validation against ANSYS and existing test results on composite beam long-term performance attests to its effectiveness in instantaneous analysis. The model predicts the time-related behavior of simply supported composite beams, highlighting significant influences of concrete shrinkage and creep on structural responses. Ting et al. [18] reviewed the performance of shear connectors in steel–concrete composites exposed to hostile environments. Despite extensive use, inefficient connectors can weaken composite structures. Various connector types' load transfer mechanisms, influences of hostile conditions like temperature and corrosion, and failure modes were evaluated, urging further research on connector deterioration. Du et al. [19] explores the shear behavior of corroded stud connectors in steel and bridge engineering. Experimental investigation reveals increased tensile deformation in corroded studs under dynamic loading, with higher strain rates enhancing shear fracture. Corrosion accelerates sensitivity to dynamic loads, yet ultimate shear stress remains unaffected.

In summary, most scholars have not considered the corrosion of connectors in the investigation of the long-term performance of composite beams. However, in practical engineering applications, corrosion of connectors is inevitable. While Zhang [7] did consider corrosion, the study only focused on the short-term flexural carrying capacity performance. Xiong et al. [8] only discussed the static performance of bolted connections after long-term load unloading due to corrosion, without addressing performance during long-term load application. Furthermore, no scholar has yet proposed an effective finite element analysis method for evaluating the long-term performance of composite beams under bolt corrosion [20]. Therefore, it is necessary to study the corrosion of connectors in composite beams. This paper investigates the long-term performance of composite beams by considering different bolt corrosion scenarios using numerical methods combined with relevant experimental data [9, 21].

2. Experiment Introduction

The long-term performance of steel–concrete composite beams was investigated by researcher Peng [9], considering different corrosion rates, presence of load, and loading age conditions. A total of 11 simply supported composite beams were designed for the experiment, divided into four categories of specimens: specimens corroded under load (SCB7∼SCB11), specimens not corroded under load (SCB2, SCB3), specimens corroded without load (SCB4, SCB5, and SCB6), and specimens not corroded without load (SCB1). Select SCB-1, SCB-2, SCB-3, SCB-4, SCB-5, SCB-7, SCB-8, and SCB-10 for numerical simulation. These specimens include both corroded and noncorroded components, with loading conditions of unloading, 7-day age loading, and 28-day age loading, in various combinations, to make the numerical simulation results more reliable. The basic parameters of the composite beams are shown in Table 1. The material parameters of the concrete test blocks from the same batch can be found in Table 2,. All experiments were conducted using C40 ordinary concrete with standard curing for 28 days, with a compressive strength not less than 40 MPa. The experiment focused primarily on the study of bolt corrosion. Using electrochemical principles, the specimens achieved the expected corrosion rate, while the maximum compressive stress σmax (at the top surface of the concrete flange at midspan) induced by long-term loading was controlled at around 0.4 fc. The long-term loading value was a concentrated load of $P = 30$ kN at midspan. The combined action of electrical corrosion and loading lasted for 225 days. The cross-sectional diagram and front view of the specimen can be seen in Figures 2 and 3.

3. Numerical Model Establishment and Theoretical Background

A numerical modeling analysis is conducted based on the corrosion of anchor bolts in commonly used composite structures. The feasibility of finite element analysis is verified by comparing the results with experimental data. On this basis, more working conditions are extended to study and

Table 2: Concrete material parameters.

Age of concrete (d)	Cube compressive strength (MPa)	Soaked cube compressive strength (MPa)	Elastic modulus (MPa)
7	32.42	—	2.97×10^4
14	37.59	—	3.10×10^4
28	46.44	—	3.35×10^4
45	46.85	44.69	3.42×10^4
90	48.34	48.08	3.63×10^4
150	49.57	50.23	3.81×10^4
225	50.40	52.30	3.91×10^4

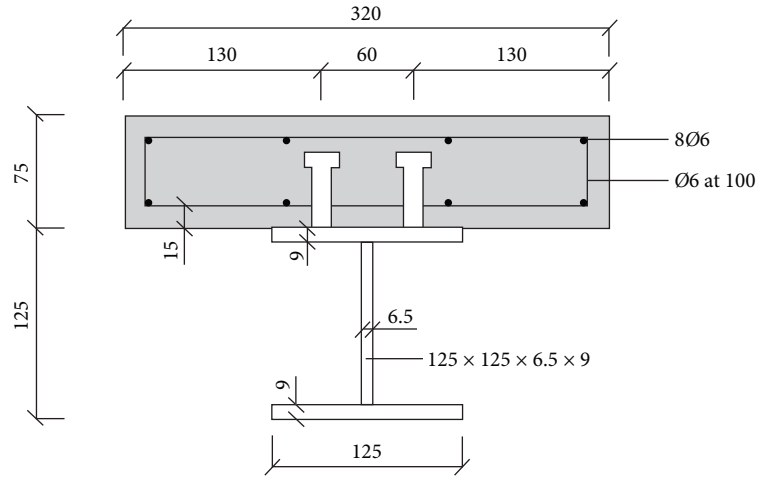

Figure 2: Sectional dimension of the specimen.

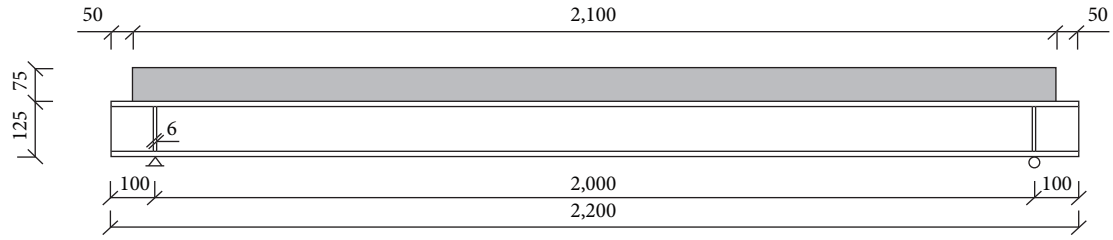

Figure 3: Frontal view of the specimen.

analyze the long-term behavior of steel–concrete composite beams with corroded anchor bolts.

3.1. Finite Element Model. In this study, a simply supported constraint is adopted for the composite beam model, and DIANA software is used for numerical simulation. At one end of the flange of the I-beam at the support location, all translational degrees of freedom are constrained (Tl = T2 = T3 = 0), while at the other end, the lateral and vertical translational degrees of freedom are constrained (T1 = T3 = 0). The self-weight of the structure is applied through a gravity field, and the long-term load is applied as a surface load on the top surface of the concrete slab (Figure 4). The finite element model is a 1:1 scale model. In the figure, some parts of the concrete slab are hidden to facilitate a better observation of the steel and bolts. Eight-node hexahedral elements (HX24L) are used to simulate the steel and concrete in the specimen model. For the concrete and steel plates, hexahedral elements are used to ensure good adaptability and convergence of the elements. Steel reinforcement beam elements are used for the anchor bolts, which are embedded in the concrete to withstand shear forces. Through simulations with various grid sizes, taking into account the analysis accuracy and computational efficiency of the model, it is finally concluded that a grid size of 20 mm achieves better accuracy and higher computational speed. The convergence criteria include force and displacement convergence, indicating convergence of the iterative calculation results as long as either force or displacement converges during the iterative process. The convergence tolerance is set to 0.01, with a maximum of 50 iterations allowed. The mesh size of the steel and concrete is set to 20 mm. The total number of solid elements is 11,742, and the total number of steel reinforcement elements is 61.

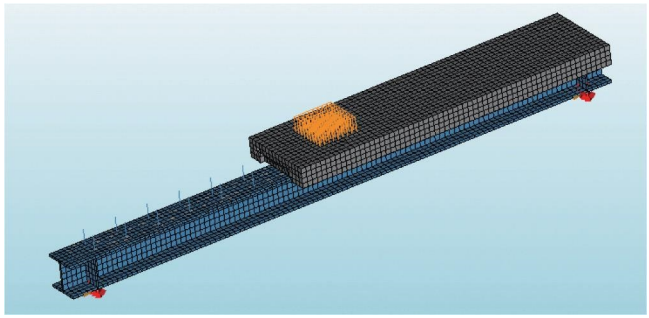

Figure 4: FE model.

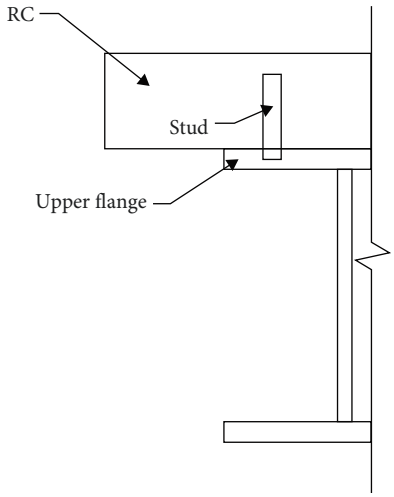

Figure 5: Embedded beam element.

3.2. Interface Element and Parameter Selection. The simulation of the interface behavior in composite beams includes two parts: the interface simulation between concrete and steel sections and the interface simulation between bolts and concrete. The interface simulation between concrete and steel sections is conducted using surface-to-surface contact elements with Coulomb friction properties. In the simulated experiments, a layer of epoxy resin is applied to the surface of the steel, resulting in minimal friction. Therefore, it can be assumed that the steel–concrete interface only provides vertical support. Hence, a large value is chosen for the normal stiffness modulus of the steel–concrete interface, while small values are selected for the two shear directions to simulate the behavior. The normal stiffness modulus of the interface between the steel and concrete is set to 2,000 N/mm^3, while the tangential stiffness modulus is set to 0.001 N/mm^3. The friction angle is set to 0.38 rad [22], and the cohesion is set to 0.001 N/mm^2. The interface element opening model selected is the gap model.

Two approaches can be used to model the interface of bolts: (1) The first one is using embedded beam elements for the bolts, as shown in Figure 5. The bolts are set as beam elements and penetrate the interface elements between the steel section and concrete, being embedded in the steel flange

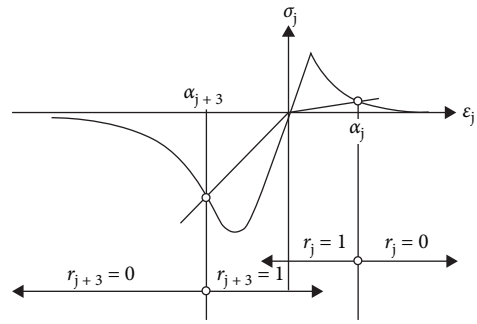

Figure 6: Total strain crack model [23].

[23]. The bolts are modeled as cylindrical geometries, and a cohesive-sliding model is applied for the interface. (2) The second one is using solid elements for the bolts, where the root of the bolt is fixed to the steel beam and other parts of the bolt are embedded in the concrete slab [24]. After modeling and analysis using both approaches, it was found that the results were consistent in terms of the long-term behavior of the composite beams (e.g., deflection–time curve). The only difference lies in the local stress distribution of the bolts. However, using discrete reinforcement elements to simulate the bolts proved to be more convenient, efficient, and significantly faster in terms of computational speed compared to using solid elements. Therefore, the later numerical analyses in this study adopted the embedded beam elements to simulate the bolts.

Embedded beam element settings: In the geometric properties setting of the anchor bolt, select the reinforcement type as circular beam bond-slip, with a diameter of 13 mm. In the data properties setting, select Bondslip Reinforcement/Foundation Pile as BEAM. Choose the interface continuity in the reinforcement properties interface, and in the analysis options under the model assessment, select to evaluate the reinforcement of the interface element. The anchor bolts do not need to be merged with the concrete nodes.

3.3. Simulation Method for Long-Term Behavior of Steel–Concrete Composite Beams. This study focuses on the long-term behavior of composite beams under normal service conditions, but localized regions in the concrete may reach the plastic stage. Therefore, the mechanical behavior of concrete is simulated using the total strain crack model [25]. The tensile curve is Hordijk's tensile softening curve, the compressive curve is Maekawa's cracking concrete curve, the tensile fracture energy is 0.1465 N/mm, and the Poisson's ratio is 0.15. Other material properties can be found in Table 2 based on experimental data. The constitutive relationship is shown in Figure 6. The constitutive model selected for reinforcing bars, structural steel, and bolts is the von Mises plastic yield model, which incorporates plastic hardening. The stress–strain curve is represented by a trilinear form, as shown in Equations (1) and (2), with material properties detailed in Table 1. The stress–strain curve is illustrated in Figure 7.

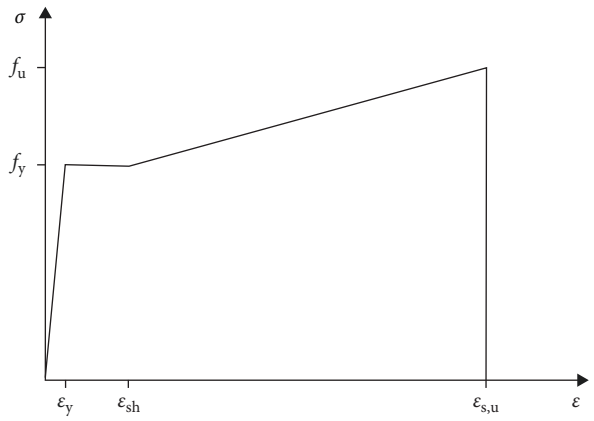

Figure 7: Stress–strain curve.

$$\sigma_s = \begin{cases} E_s\varepsilon & 0 \le \varepsilon < \varepsilon_y \\ f_y & \varepsilon_y \le \varepsilon < \varepsilon_{sh} \\ f_y + E_s'(\varepsilon - \varepsilon_{sh}) & \varepsilon_{sh} \le \varepsilon \le \varepsilon_{s,u}, \end{cases} \quad (1)$$

$$E_s' = \frac{f_u - f_y}{\varepsilon_{s,u} - \varepsilon_{sh}}. \quad (2)$$

In the above equation, f_y andε_y represent the yield strength and yield strain, respectively, while ε_{sh} denotes the end strain of the yield plateau, with a value of 0.025. f_u and $\varepsilon_{s,u}$ represent the ultimate strength and ultimate strain, respectively, with $\varepsilon_{s,u}$ set to 0.15. E_s represents the elastic modulus of the reinforcing bars, while E_s' represents the linear slope of the reinforcing bars in the strain-hardening stage, calculated using Equation (2).

The simulation method for the long-term behavior of composite beams is as follows:

(1) Calculation Method of Shrinkage and Creep in Standards (referred to as Standard Creep Method, SCM). The standard method considers two types of shrinkage in concrete [5, 26]. One type is inherent autogenous shrinkage, which is caused by the volume of cement hydration products being smaller than the volume of cement and water involved in the hydration reaction. The autogenous shrinkage curve is shown in Figure 8. The other type considered is drying shrinkage, which occurs when the distance between gel particles in the hydrated cement paste is less than the thickness of 10 water molecules, which leads to a tensile force generated by adsorbed water molecules to balance the molecular attraction between the particles, resulting in volume expansion [27]. Hence, the loss of this adsorbed water in drying will instead cause volume shrinkage. The shrinkage curve is shown in Figure 9 [28].

In the standard method, the concrete creep model adopts the Kelvin chain model [29]. A Kelvin element consists of an elastic component and a viscous component connected in parallel. Its physical significance can be described as a series

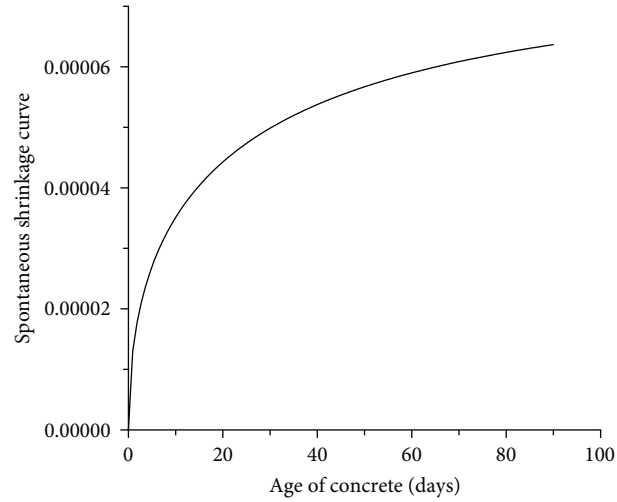

Figure 8: Spontaneous shrinkage curve.

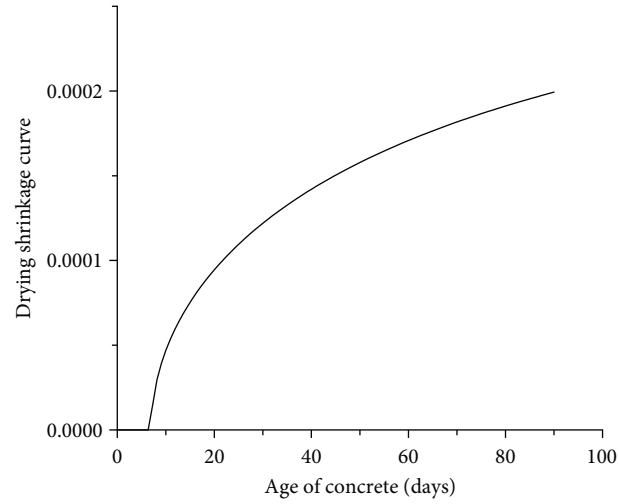

Figure 9: Drying shrinkage curve.

of interconnected elastic components (springs) and viscous components (dampers). This is shown in Figure 10. E_n represents the elastic modulus of the nth Kelvin element, and ηn represents the viscous damping coefficient of the nth Kelvin element. The Kelvin chain is formed by connecting multiple Kelvin elements in series. The Kelvin chain is based on the aging theory of concrete and is often used to analyze time-dependent problems in reinforced concrete structures. The elastic modulus of concrete in the Kelvin chain is one of its important parameters, which is closely related to the age of the element, temperature, and humidity.

(2) The defined modulus method (DMM) is used to account for the variation in normal stiffness modulus at the interface between corroded anchor bolts and concrete. After long-term corrosion, gaps exist at the interface between the anchor bolt and concrete, resulting in a decrease in interface stiffness. This leads to additional deflection in the composite beam. When linked with the degree of corrosion, the normal

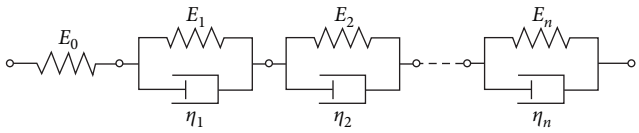

Figure 10: Kelvin element chain [25].

stiffness modulus then can be referred to for the study of the time-dependent behavior of corroded anchor bolts in composite beams.

4. The Numerical Comparative Study on the Long-Term Performance of Composite Beams Considering the Influence of Corroded Force on Interface Stiffness

Based on the experimental data from the reference [2], a study is conducted using different methods to simulate the long-term behavior of composite beams.

In the analysis using the SCM, many researchers adopted a multi-Kelvin element model to fit the experimental data. Due to its ability to capture both elastic and creep deformation which has a stable limit, the three-parameter model [25] is suitable for components with initial elastic deformation that undergo long-term sustained loading. Therefore, this study selects the three-parameter Kelvin model, which consists of an elastic component and a Kelvin element connected in series. The three parameters are denoted as E0, E1, $\tau 1$, and τ represents the time damping, where $\tau = \eta/\mathrm{E}$.

In the research utilizing the DMM to supplement the simulation of the corrosion effect on anchor bolts, the normal stiffness modulus is defined as the ratio of normal stress to normal relative displacement. After anchor bolt corrosion, the diameter of the anchor bolt decreases, and therefore, the relative displacement is considered with respect to the reduction in diameter (Δd). As steel reinforcement corrosion can cause rust expansion stress [20], the curve of rust expansion stress with respect to Δd is shown in Figure 11. The peak rust expansion force is calculated using the following formula: $P = f_t\ (0.94\,c/d + 0.91)$ [20], where c is the thickness of the protective layer and d is the diameter of the anchor bolt. The normal stress after corrosion is determined by the initial normal stress and the rust expansion stress, thus determining the corresponding normal stiffness modulus in the corroded state. The deflection cloud diagram of the composite beam under long-term load simulated using the DMM is shown in Figure 12.

The comparative results are shown in Figure 13. SCB-1, SCB-4, and SCB-5 represent unloaded specimens, while the rest are loaded specimens. SCB-1, SCB-2, and SCB-3 are specimens without corrosion. When only concrete shrinkage and creep occur but without corrosion, the simulation results of both methods align closely and are represented by the same line. Table 3 presents the comparison between the long-term deflection (in millimeters) calculated by the two methods and the experimental results for a 225-day loading period. Currently, in China, when simplifying calculations

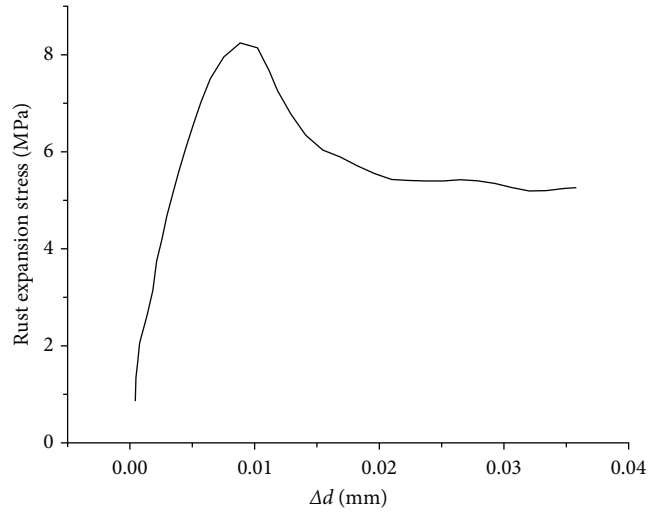

Figure 11: Variation curve of rust expansion force with Δd.

for long-term deformations of composite structures, it is common practice to reduce the long-term elastic modulus of concrete. According to the "Code for Design of Steel Structures," the long-term elastic modulus of concrete is specified to be half of the initial elastic modulus, while in the "Code for Design of Highway Bridges and Culverts Steel Structures," it is taken as 0.4 times the initial elastic modulus. This paper will adopt the recommended reduction values from the "Code for Design of Steel Structures" to calculate the development of concrete strain and compare it with experimental measurements, simulation values, and the calculated values obtained from the formula proposed by researcher Peng [9], as shown in Table 3 for comparison.

From Figure 13, it can be observed that the DMM yields good agreement with the experimental results for all loading conditions, as it takes into account the influence of anchor bolt corrosion on stiffness and long-term deflection. On the other hand, when simulating using the SCM, the results deviate significantly from the experimental data under the corroded condition and only align well in the absence of corrosion, though not as well as the DMM method.

The reason for this difference is that the deflection of the composite beam is influenced by both concrete shrinkage and creep, and the effect of anchor bolt corrosion on long-term deflection needs to be considered. In the unloaded state, although the anchor bolts experience corrosion, the creep caused by their self-weight is relatively small compared to the influence of concrete shrinkage. Therefore, the error of the SCM method is relatively small. However, when considering loaded conditions, the failure to account for the effects of corrosion leads to larger deviations.

Currently, the calculation method for the long-term deflection of steel–concrete composite beams is based on the principle of effective modulus method. This method involves reducing the elastic modulus of concrete after long-term loading, thereby increasing the ratio of elastic modulus between steel and concrete. The calculation is performed using the formula for elastic deflection [1]. However, this method can only be applied to noncorroded components, and it cannot be used

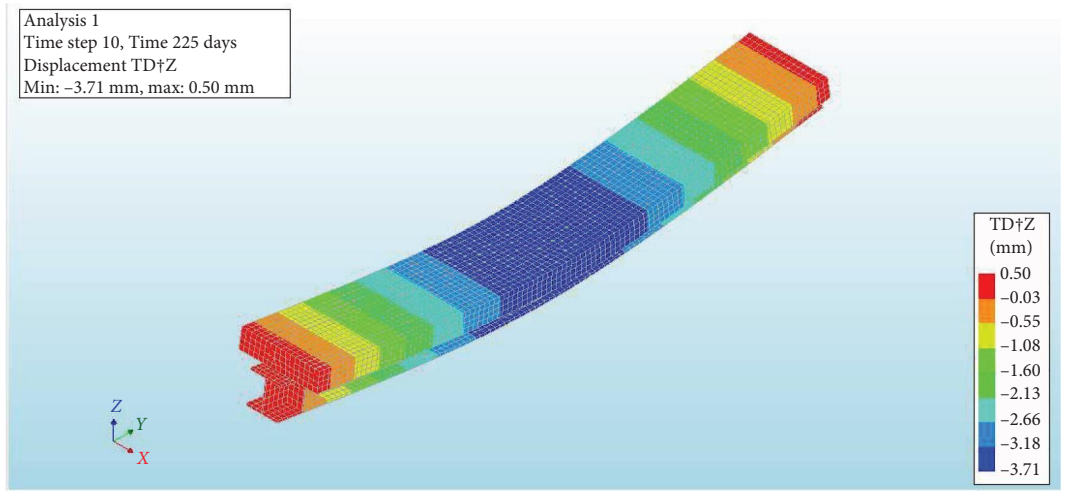

(a)

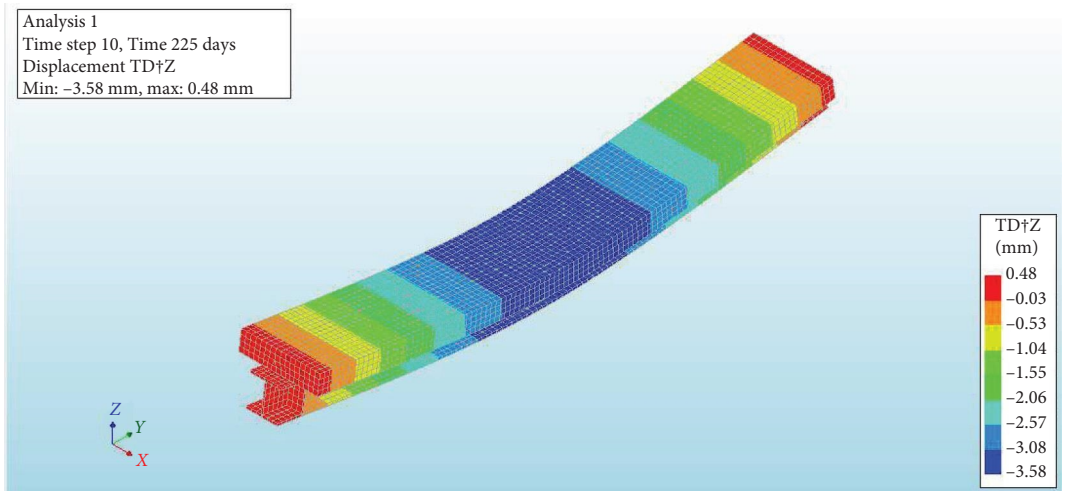

(b)

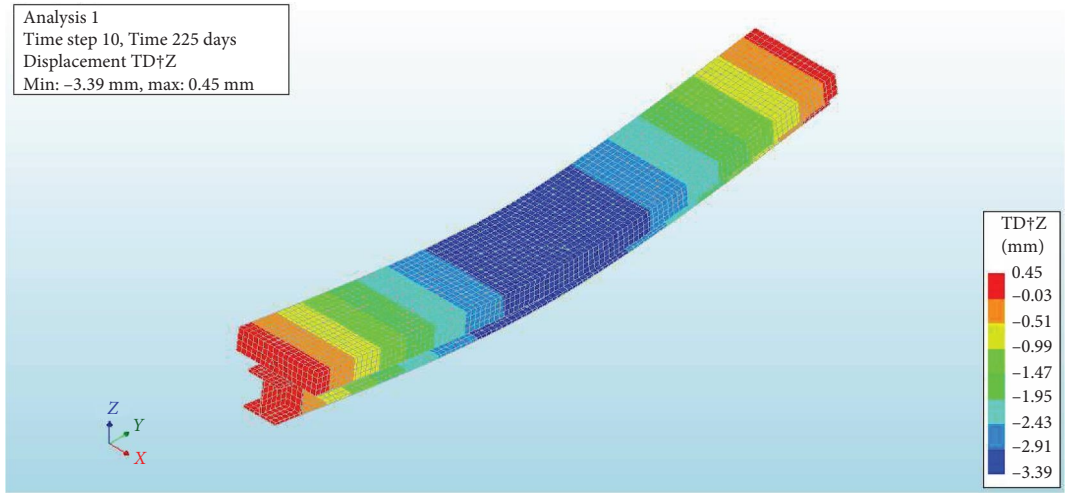

(c)

Figure 12: Contour plot of the simulated deflection of the loaded specimens (using the defined modulus method (DMM)). (a) Deflection of the loaded specimen at a 7-day age (corrosion rate: 7.03%, SCB-8). (b) Deflection of the loaded specimen at a 7-day age (corrosion rate: 5.08%, SCB-7). (c) Deflection of the loaded specimen at a 28-day age (corrosion rate: 6.25%, SCB-10).

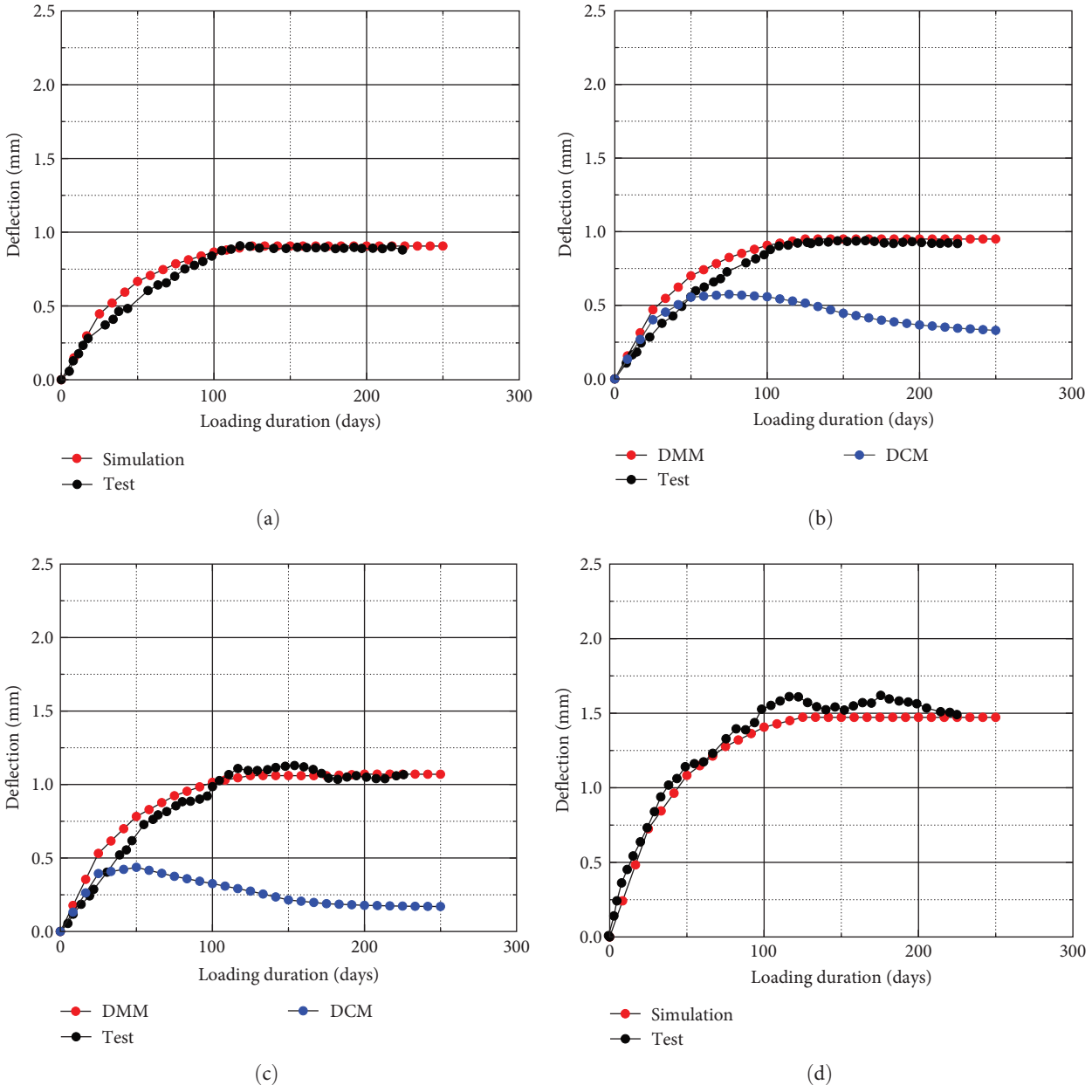

Figure 13: Continued.

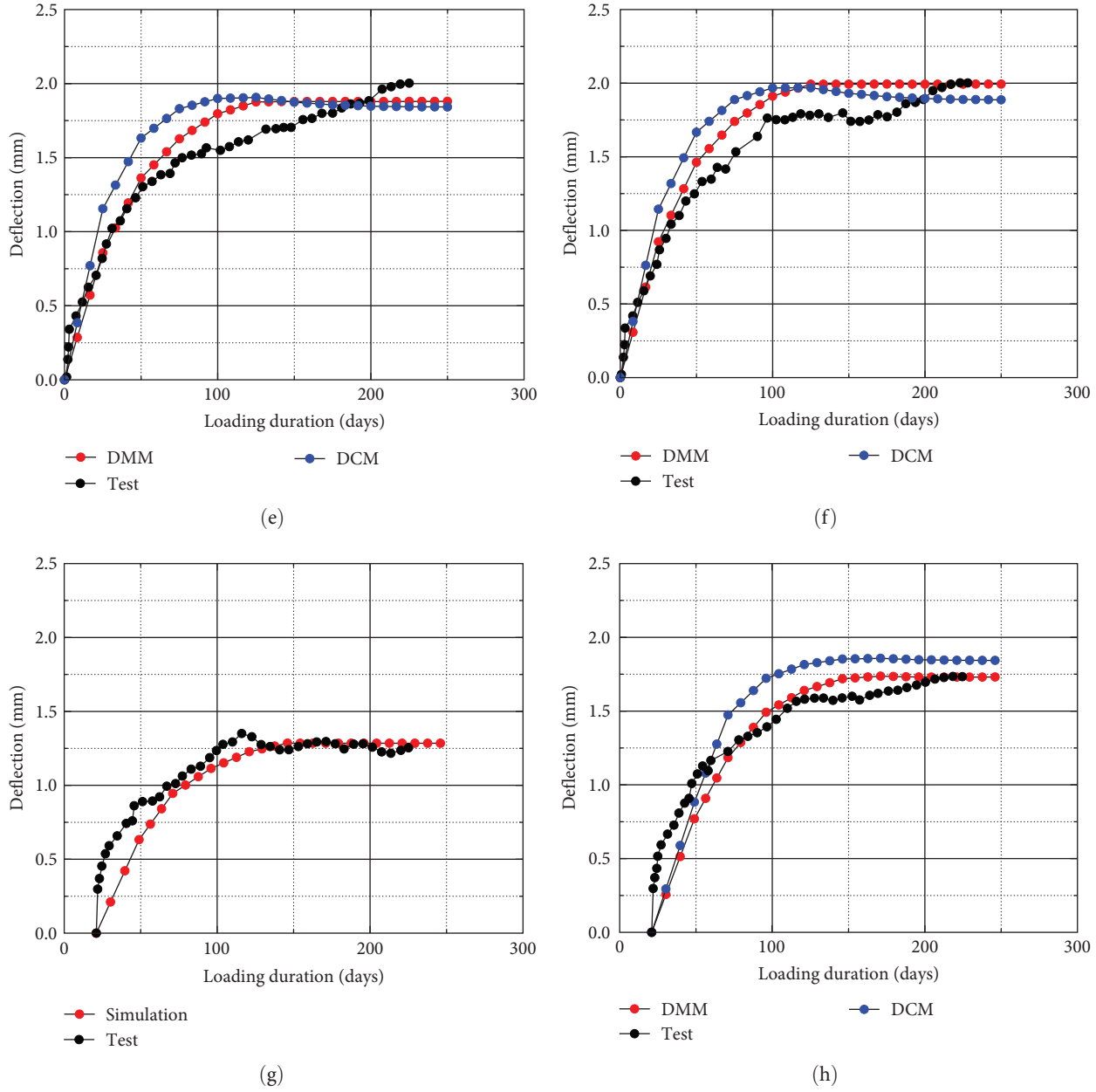

Figure 13: Time–deflection relationship of the corroded anchor bolt composite beams. (a) Unloaded specimen without corrosion (SCB-1). (b) Unloaded specimen (corrosion rate: 3.81%, SCB-4). (c) Unloaded specimen (corrosion rate: 9.77%, SCB-5). (d) Loaded specimen at a 7-day age (without corrosion, SCB-2). (e) Loaded specimen at a 7-day age (corrosion rate: 5.08%, SCB-7). (f) Loaded specimen at a 7-day age (corrosion rate: 7.03%, SCB-8). (g) Loaded specimen at a 28-day age (without corrosion, SCB-3). (h) Loaded specimen at a 28-day age (corrosion rate: 6.25%, SCB-10).

to calculate deflection for corroded components. The calculation of effective modulus values is related to the creep coefficient. The creep models in CEB-FIP 1990 and ACI 209R perform well. Therefore, in this study, the deflection of noncorroded components (SCB-1, SCB-2, and SCB-3) is calculated using the effective modulus method combined with the creep models from these two standards. The results are as shown in Table 3.The calculation results indicate that there is a significant discrepancy between the calculated values from CEB-FIP 1990 and the experimental values, suggesting an overly conservative approach. On the other hand, the calculated values from ACI 209R are close to the experimental values. Therefore, for noncorroded components, the ACI 209R code can be adopted for calculation.

In both DMM and SCM methods, the results from the DMM are closest to the measured values, with very small relative errors. Therefore, using DMM can provide better simulation. The SCM is more suitable for conditions where the anchor bolts are not corroded under long-term loading. The proposed DMM in this study is applicable to the study of concrete shrinkage and creep under both loaded and unloaded conditions. Moreover, it takes into account the corrosion of

Table 3: Comparison of long-term deflections (mm) between the loaded specimens at the 225th day.

	Unloaded specimen without corrosion			Loaded specimen at a 7-day age			Loaded specimen at a 28-day age	
Specimen number	SCB-1	SCB-4	SCB-5	SCB-2	SCB-7	SCB-8	SCB-3	SCB-10
Actual corrosion rate (%)	0	3.81	9.77	0	5.08	7.03	0	6.25
Long-term deflections	0.879	0.918	1.067	1.490	2.002	2.001	1.253	1.733
SCM	0.906	0.329	0.169	1.472	1.842	1.886	1.284	1.843
Relative error (%)	3.02	−64.13	−84.10	−1.23	−8.01	−5.74	2.50	6.35
DMM	0.906	0.949	1.069	1.472	1.880	1.993	1.284	1.730
Relative error (%)	3.02	3.35	0.27	−1.23	−6.10	−0.39	2.50	−0.15
CEB-FIP 1990	0.63	—	—	1.18	—	—	1.14	—
Relative error (%)	−28.41	—	—	−20.81	—	—	−8.80	—
ACI 209R	0.93	—	—	1.45	—	—	1.28	—
Relative error (%)	5.8	—	—	−2.68	—	—	2.15	—
Peng [9] calculated values	0.99	1.04	1.18	1.64	1.89	2.16	1.34	1.85
Relative error (%)	12.50	13.04	13.04	13.04	−5.50	8.00	7.20	6.94

anchor bolts and its impact on the long-term behavior of composite beams. Therefore, the subsequent numerical studies in this paper will be conducted using the DMM.

5. The Impact of Load Strength, Bolt Corrosion Rate, and Bolt Diameter on the Long-Term Behavior of Composite Beams

5.1. Influence of Anchor Bolt Corrosion on the Long-Term Behavior of Composite Beams under Different Loading Strengths. Considering the limited number of specimens and the limited variation in load levels and anchor bolt corrosion on the long-term behavior of composite beams under sustained loading conditions, to further improve the analysis, a numerically validated method is used to supplement the experimental study and investigate the long-term deformation capacity of steel–concrete composite beams under more levels of anchor bolt corrosion and loading strengths. Through numerical analysis, it was found that when the corrosion rate exceeds 15%, the deflection of the composite beam is almost identical to that of a composite beam without bolts, indicating bolt failure. This finding is consistent with the conclusion reached by Zhang [7] in the study of the flexural load-carrying capacity of corroded bolted composite beams, where it was suggested that bolt failure occurs when the corrosion rate exceeds 13%. Therefore, the parametric analysis in this section will focus on studying the deflection for corrosion rates ranging from 5% to 15%, which is also the range studied by most scholars.

Figure 14 depicts the variation of midspan deflection with time under different loading strengths. The deflection of the composite beam increases with increasing duration under different levels of anchor bolt corrosion and tends to stabilize at various loading strengths. The larger the load, the more significant the variation of deflection with the rust rate. This means that the range between 5% rust rate and 15% rust rate, as shown in the graph, is wider. It indicates that under the coupled effect of load and rust rate, the deflection of composite beams will increase significantly. As shown in

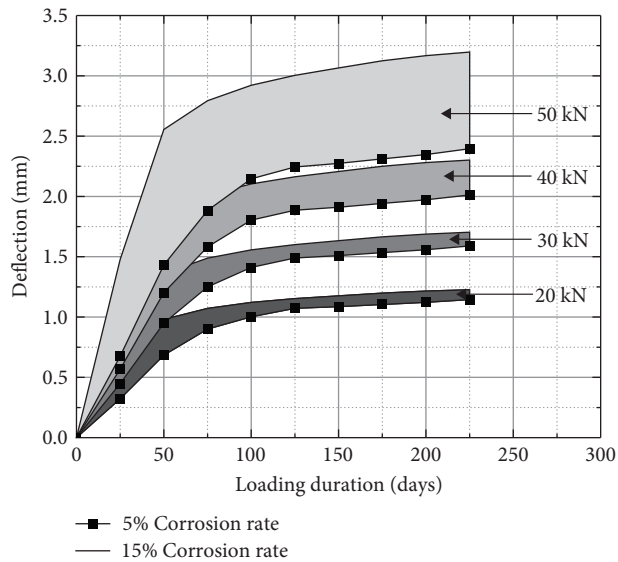

Figure 14: Deflections of anchor bolts under different corrosion rates and loading strengths.

Table 4, at 225 days, under a load level of 20 kN, the increase is 105.42%, while under a load level of 50 kN, the increase reaches 131.41%. However, as the loading strength increases, the increase in deflection with time becomes more significant within the same range of corrosion rate limits. The relationship between deflection and corrosion rate for the same load but different corrosion rates is shown in Table 4.

Figure 15 illustrates the variation of deflection of a loaded specimen at a 7-day age (corrosion rate: 7.5%) under different loading durations. From the results, it can be observed that the deflections almost follow a linear relationship with load changes for the same duration. Moreover, as the loading duration increases, the increases in the deflections become smaller and tend to reach a stable value. It can be observed that from 100 days onward, the magnitude of deflection change decreases significantly. This is because shrinkage

Table 4: Deflection relationship for the same load at different corrosion rates.

Long-term loading (kN)	Levels of anchor bolt corrosion	Loading duration (days)								
		20	50	75	100	125	150	175	200	225
20	5%	0.32	0.68	0.9	1	1.07	1.09	1.1	1.12	1.14
	15%	0.55	0.93	1.01	1.1	1.14	1.16	1.18	1.19	1.21
	Increase	169.35%	135.96%	112.45%	109.82%	106.53%	106.37%	106.72%	106.25%	105.42%
30	5%	0.45	0.95	1.25	1.41	1.49	1.51	1.53	1.56	1.59
	15%	0.79	1.36	1.49	1.56	1.6	1.63	1.67	1.69	1.7
	Increase	175.54%	143.27%	119.11%	110.28%	107.46%	108.21%	108.53%	108.33%	107.17%
40	5%	0.57	1.2	1.58	1.8	1.89	1.91	1.94	1.97	2.01
	15%	1.06	1.84	2.01	2.1	2.16	2.21	2.25	2.28	2.3
	Increase	187.40%	152.95%	127.16%	116.67%	114.72%	115.52%	115.86%	115.65%	114.41%
50	5%	0.68	1.43	1.88	2.15	2.24	2.27	2.31	2.35	2.4
	15%	1.19	2.19	2.62	2.88	3	3.02	3.06	3.1	3.15
	Increase	176.49%	152.86%	138.89%	134.23%	133.54%	132.73%	132.40%	132.07%	131.41%

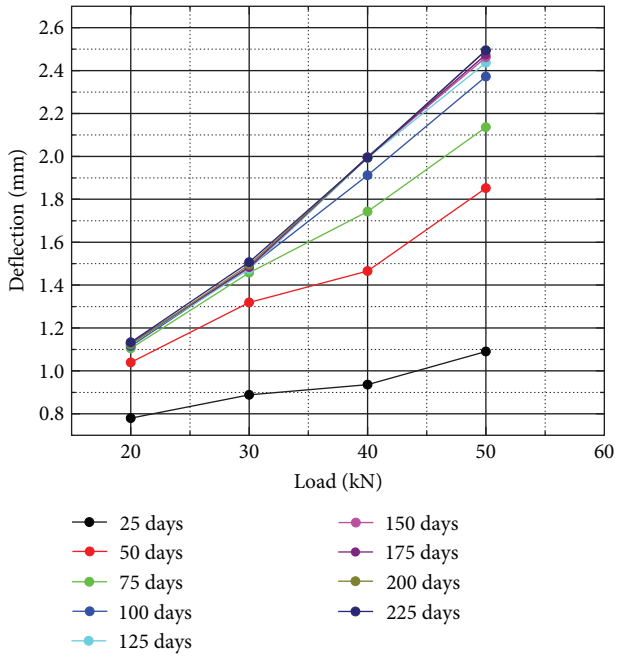

Figure 15: Load–deflection graph of the loaded specimen at a 7-day age (corrosion rate: 7.5%).

and creep mainly occur within the first 100 days, while the variation in deflection after 100 days is primarily due to the slow growth of creep and the effects of bolt corrosion.

Table 5 presents the deflection (mm) and its rate of change under different loads at a corrosion rate of 7.5%. It reflects the relationship between anchor bolt corrosion rate and deflection, which shows a significant linear growth. This indicates that the corrosion rate has a notable impact on the long-term deflection of composite beams. As the number of loading days increases, the rate of change also increases. This is because the corrosion rate varies with the number of loading days. At the beginning of loading, the corrosion rate is 0%. However, as the number of loading days reaches 225 days, the corrosion rate gradually increases to 7.5%. The coupling effect of corrosion and load becomes more severe, leading to an increase in the rate of change.

Figure 16 illustrates the variation of deflection with loads for different corrosion rates. As shown in the figure, the deflection increases approximately linearly with increasing corrosion rate under long-term sustained loading. Additionally, at high load levels, the change in deflection with corrosion rate is more significant compared to the low load conditions, indicating that corrosion rate has a larger impact on deflection under high load conditions but a smaller impact under low load conditions.

5.2. Influence of Different Bolt Diameters on the Long-Term Deflection of Composite Beams under Varying Corrosion Rates. As bolt diameter serves as a prominent parameter in the research conducted by numerous scholars on composite beams, this section will investigate the influence of bolt diameter on the long-term deflection of composite beams under bolt corrosion conditions. Currently, bolt specifications include φ8, φ10, φ13, φ16, φ19, φ22, φ25, and φ28, totaling eight types. The research results for these eight bolt specifications are as follows.

From Figure 17, it can be observed that under different corrosion rates, the trend of long-term deflection with bolt diameter remains relatively consistent. However, as the bolt diameter increases, the long-term deflection actually increases. This is because under normal operating conditions, for the same corrosion rate, a larger bolt diameter results in a greater reduction in effective cross-sectional area, thereby leading to an increase in long-term deflection. This does not imply that larger bolt diameters are inherently undesirable. In practical engineering, under the same corrosion environment, it takes more time for a larger diameter bolt to reach the same corrosion rate as a smaller diameter bolt. It is important to

Table 5: Deflection (mm) and rate of change for the specimen under different loads at a corrosion rate of 7.5%.

Loading duration (days)	Load						
	20 kN	30 kN		40 kN		50 kN	
	Deflection	Deflection	Rate of change (%)	Deflection	Rate of change (%)	Deflection	Rate of change (%)
25	0.78	0.89	113.89	0.94	105.36	1.09	116.49
50	1.04	1.32	126.87	1.47	111.11	1.85	126.39
75	1.11	1.46	131.90	1.74	119.54	2.14	122.57
100	1.12	1.48	132.92	1.91	128.99	2.37	124.07
125	1.13	1.47	130.79	1.99	135.22	2.44	122.25
150	1.13	1.48	131.53	2.00	134.46	2.46	123.33
175	1.13	1.48	131.60	2.00	134.60	2.47	123.92
200	1.12	1.49	132.92	1.99	133.35	2.49	125.15
225	1.13	1.51	132.95	1.99	132.34	2.49	125.06

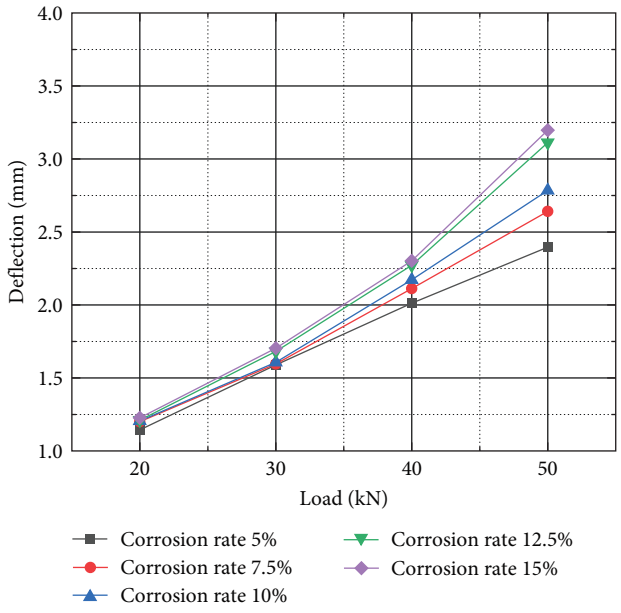

Figure 16: Load–deflection relationship (at the 225th day).

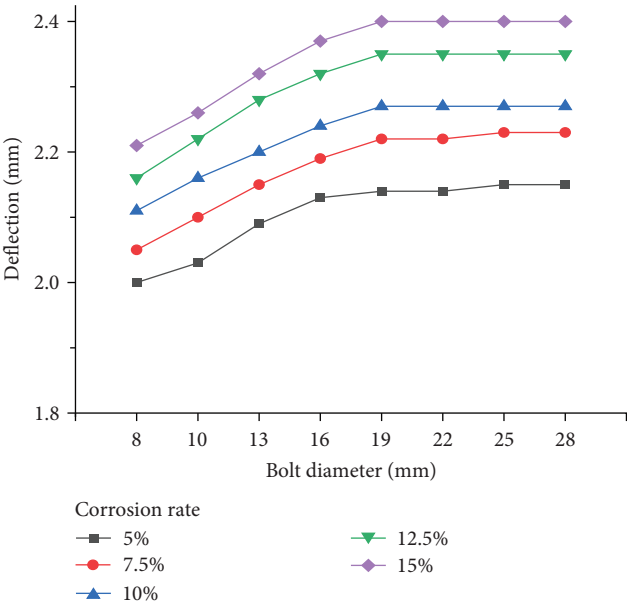

Figure 17: Graph showing the variation of deflection with bolt diameter under different corrosion rates.

determine the bolt diameter based on actual engineering conditions and to implement effective corrosion prevention measures.

6. Conclusions and Future Perspectives

In this study, the defined creep method (DCM) and DMM were used to simulate eight tested specimens from previous research, analyzing the long-term behavior of steel–concrete composite beams with anchor bolts having different corrosion rates and loading ages. The results indicate that the DMM can effectively simulate the long-term deflection of composite beams. The DCM is suitable for simulating the long-term deflection of composite beams under loading conditions, but it fails to model the deflection under self-weight conditions, showing a deviation of over 60% from the experimental values. By using the DMM, the long-term deflection of composite beams under various corrosion rates and loading levels was studied. For every 10 kN increase in load, the deflection increased by 10%–35% compared to the previous load level. When the increment of corrosion rate was the same, the higher the load, the greater the influence of corrosion rate on deflection.

The corrosion rate of the bolts simulated in this study ranges from 5% to 15%, targeting simply supported steel–concrete composite beams under low corrosion rates. Through numerical analysis, it was found that when the corrosion rate exceeds 15%, the bolts begin to enter a failure state. This study did not delve further into this aspect. It is hoped that researchers will conduct experimental studies on the failure of bolts under high corrosion rates. Additionally, further analysis and validation are needed for the long-term performance of continuous beams with multiple spans. The long-term deflection calculation method for composite beams considering anchor bolt corrosion can be proposed based on the DMM. This study only focused on the long-term deflection under normal service conditions, and further research is needed to investigate the

ultimate limit state of composite beams with anchor bolts subjected to long-term corrosion.

Data Availability

The data that support the findings of this study are available in [9].

Conflicts of Interest

The authors declare that they have no conflicts of interest.

References

[1] X. Wang, R. Song, Y. Zhan, and R. Zhao, "Simulation and calculation method of long-term behavior of steel–concrete composite beams," *Industrial Construction*, vol. 50, no. 4, pp. 132–137, 2020.

[2] W. Ji, Q. Bai, and K. Luo, "Deflection analysis of steel–concrete composite girders with different boundaries under long-term effects," *Journal of Harbin Engineering University*, vol. 44, no. 3, pp. 434–442, 2023.

[3] C. Han, *Theoretical and experimental research on creep and shrinkage effect of steel and concrete composite beams*, Ph.D. thesis, Kunming University of Science and Technology, 2016.

[4] J. Fan, J. Nie, and H. Wang, "Long-term behavior of composite beams with shrinkage, creep and cracking I: experiment and calculation," *China Civil Engineering Journal*, vol. 42, no. 3, pp. 8–15, 2009.

[5] J. Fan, X. Nie, Q. Li, and Q. Li, "Long-term behavior of composite beams under positive and negative bending. II: analytical study," *Journal of Structural Engineering*, vol. 136, no. 7, pp. 858–865, 2010.

[6] W. Di, *Study on the influence of concrete shrinkage and creep on the long-term performance of steel–concrete composite beam bridges*, M.S. thesis, Harbin Institute of Technology, 2018.

[7] H. Zhang, *Numerical simulation and analysis of the bending performance of bolted corroded steel–concrete composite beams*, M.S. thesis, Hunan University of Science and Technology, 2016.

[8] H. Xiong, L. Yang, and G. Cao, "Experimental study on the static behavior of corroded bolted connections under long-term load after unloading," *Journal of Railway Science and Engineering*, vol. 15, no. 6, pp. 1524–1533, 2018.

[9] P. Peng, *Long-term mechanical properties of steel–concrete composite beam subjected to corrosion and loading*, M.S. thesis, Xiangtan University, 2020.

[10] H. Xiao, "Model test study on shear behavior of welded stud connectors in corrosive environment," *Journal of Highway and Transportation Research and Development*, vol. 40, no. 9, pp. 135–140+150, 2023.

[11] L. Wang, H. Wei, Y. Gao, W. Ren, and X. Wei, "Analysis of shear resistance of stud connectors under different levels of corrosion," *Journal of Shenzhen University (Science & Engineering)*, vol. 41, no. 1, pp. 58–65, 2024.

[12] Z. Wang, *PBL shear in steel–concrete composite beams under strong decay study on mechanical properties of force connectors*, M.S. thesis, Xi'an Technological University, 2023.

[13] K. Wang, X. Liu, and B. Wang, "Analysis of factors influencing the post-fatigue bending capacity of composite beams with corroded bolts," *Journal of Ningbo University (Natural Science & Engineering Edition)*, vol. 36, no. 5, pp. 51–57, 2023.

[14] G. You, F. Li, Q. Zhang, Q. Wang, and T. Han, "Long-term performance of two-span continuous steel-recycled concrete composite beams," *Industrial Construction*, vol. 53, no. 5, pp. 124–131, 2023.

[15] Z. Zhang, Y. Liu, J. Liu, G. Xin, G. Long, and T. Zhang, "Experimental study and analysis for the long-term behavior of the steel–concrete composite girder bridge," *Structures*, vol. 51, pp. 1305–1327, 2023.

[16] H. Nan, P. Wang, Q. Zhang, D. M. Meng, and Q. Lei, "Study on the mechanical properties of continuous composite beams under coupled slip and creep," *Materials*, vol. 16, no. 13, Article ID 4741, 2023.

[17] G.-Y. Zhao, W. Liu, R. Su, and J.-C. Zhao, "A beam finite element model considering the slip, shear lag, and time-dependent effects of steel–concrete composite box beams," *Buildings*, vol. 13, no. 1, Article ID 215, 2023.

[18] M. Z. Y. Ting and T. Z. H. Ting, "Deterioration of structural shear connectors in steel–concrete composite exposed to hostile service environments," *Journal of Building Engineering*, vol. 73, Article ID 106690, 2023.

[19] H.-H. Du, Z.-K. Fan, W. He, and J.-Y. Pan, "Experimental investigation on corroded stud connectors under strain rates effect," *Alexandria Engineering Journal*, vol. 82, pp. 298–303, 2023.

[20] Z. Hu, L. L. Xia, C. Cheng, B. Li, and B. Xu, "Investigation on corrosion-induced cracking and corrosion expansive pressure in reinforced concrete members," *Journal of Harbin Institute of Technology*, vol. 52, no. 3, pp. 99–105, 2020.

[21] G. Zhao, T. Xiang, T. Xu, and Y. Zhan, "Stochastic analysis of shrinkage and creep effects in steel–concrete composite beams," *Journal of Computational Mechanics*, vol. 31, no. 1, pp. 67–71, 2014.

[22] L.-H. Chen, S.-T. Li, H.-Y. Zhang, and X.-F. Wu, "Experimental study on mechanical performance of checkered steel-encased concrete composite beam," *Journal of Constructional Steel Research*, vol. 143, pp. 223–232, 2018.

[23] S. Chai, *Diana 10.1 Finite Element Analysis in Civil Engineering*, Nanjing University Press, 2018.

[24] B. Shi, *Long-term behaviour of prefabricated timber-concrete composite beams*, Ph.D. thesis, Southeast University, 2021.

[25] W. Xue, T. Sun, and T. Liu, "Experimental study on prestressed steel–concrete composite beams for urban light rails under sustained loads of two years," *China Civil Engineering Journal*, vol. 46, no. 3, pp. 110–118, 2013.

[26] W. Tan and L. Da, "Study on non-linear deflection of composite steel–concrete beams," *Engineering Mechanics*, vol. S1, pp. 107–110+136, 2008.

[27] W. Zhang and Q. Yang, "Review on shrinkage of concrete," *Low Temperature Architecture Technology*, vol. 5, pp. 4–6, 2003.

[28] fib, "The *fib* model code for concrete structures 2010," Wiley-VCH Verlag GmbH & Co. KGaA, 2013.

[29] W. Xue, M. Ding, C. He, and J. Li, "Long-term behavior of prestressed composite beams at service loads for one year," *Journal of Structural Engineering*, vol. 134, no. 6, pp. 6–930, 2008.